Prediction of Energy of Interaction among Tethered Polymer Chains Confined between Two Parallel Plates

Juedu Austine and Vinay A. Juvekar*

Department of Chemical Engineering, Indian Institute of Technology Bombay, Powai, Mumbai 400 076, India

Received August 16, 2004; Revised Manuscript Received February 19, 2005

ABSTRACT: A mean field continuum model has been used to predict the free energy of interaction between the layers of polymer chains grafted on two plane parallel plates. Four cases are considered: (a) a single plate with tethered chains, (b) two plates with equal amount of tethered chains on both plates, (c) tethering only on one plate, the other plate being bare, and (d) tethered loops on two plates. The predicted force−distance profiles are compared with the experimental data, reported in the literature, on interaction of polystyrene chains grafted on mica surface, with toluene as the solvent. The tethered amount is estimated from the regression of the experimental data. The predicted and the experimental profiles are in good agreement except for the case of short tethered loops. Moreover, in the experiment where the tethered amount is reported, the regression estimate closely matches with the actual value. In the cases where the tethered amount is not reported, the estimates of the same show the correct trend. Moreover, the estimated critical distance between the plates at which the tethered layers begin to interact also matches with the experimentally measured values. The present continuum model correctly accounts for the stiffness of the polymer chain and the difference in the size of the Kuhn segment and the solvent molecule. The predictions of the present theory are compared with those of the SCF lattice model of Scheutjens and Fleer.

Introduction

Colloidal stabilization is one of the most important applications of polymer adsorption. To qualify as a stabilizing agent, the adsorbed polymer needs to form a thick layer around the colloid particles. This layer produces a strong repulsive energy barrier, which prevents the particles from approaching one another. Also, good solvent condition is necessary to prevent interpenetration of chains. In principle, surface-active polymers under good solvent condition could be good dispersing agents. However, they suffer from some serious drawbacks. The good solvent condition prevents high surface coverage by the polymer due to intersegmental repulsion. These unoccupied sites on the surface are prone to bridging by the long chains on the other particles, leading to flocculation.[1] However, if shorter chains are used to prevent bridging, a thinner adsorbed layer with weak repulsive barrier results. One way of overcoming this difficulty is to end-graft (tether) to the surface the polymer chains which have otherwise no affinity for the surface. This not only produces a dense layer with high surface coverage but also prevents the polymer chains from migrating out from the particle surface.

Two types of approaches are commonly followed to form polymer chains tethered on to a surface viz. chemical grafting of chains having reactive chain ends and physical grafting. To achieve the latter, block copolymer with one highly surface-active block is adsorbed from a selective solvent on to the surface. Taunton et al.[2] have compared the energy of interaction between two plates bearing end grafted polystyrene prepared by the above two methods and shown that both these methods of tethering have the same effectiveness. The most commonly used diblock copolymer is PEO-*b*-PS, with a short block of PEO.[2−4] Some other examples are PVP-*b*-PS[5] and PtBS-*b*-NaPSS.[6] Triblock polymers can also be used as grafting polymers. For example, Patel and Tirrel have studied compression of an adsorbed layer of a triblock copolymer, PVP-*b*-PS-*b*-PVP, from toluene, on a mica surface.[7] Here, both ends of a polymer chain are strongly adsorbed to mica, thus forming a loop.

One way of understanding the behavior of grafted chains is to evaluate the total free energy of the system of two surfaces having grafted layers of chains, as a function of distance between them as they approach each other. This free energy depends on several factors such as the entropy of the chains and the solvent molecules, the energy of interaction between the polymer and solvent, and that between the polymer and the surface, and most importantly, the total amount of chains grafted on to the surface. If the energy of interaction between the chains and the solvent is attractive (i.e., corresponds to good solvent condition), the chain conformation results in a brush. If the interaction is poor, the structure of chains becomes rather squeezed. Accordingly, the layer thickness varies, and so is the distance of closest approach. Powerful experimental techniques like surface force apparatus (SFA) make this measurement of the force of interaction possible with less than one $\mu N \cdot m^{-1}$ precision. Two types of profiles are generally observed during compression of polymer chains viz. one which is monotonically repulsive, and the other with an attractive minimum. The latter is generally caused by bridging of chains between the particles.[8,9]

Many theories, including scaling theories and self-consistent field (SCF) theories have tried to model the tethered chains. Scaling theories[10,11] consider polymer brushes that are highly stretched in good solvent conditions. The free energy associated with the chains

* Corresponding author. E-mail: vaj@che.iitb.ac.in.

10.1021/ma048319h CCC: $30.25
Published on Web 03/30/2005

has two contributions—one arising from the osmotic interaction and the other from the elastic energy of the stretched chains. The total free energy is minimized to determine the optimal values of the each contribution. Lattice based numerical SCF theory[12−16] makes use of method by Scheutjens and Fleer.[17] Analytical SCF models[18−20] use strong stretching limit. The lattice SCF results have been compared with Monte Carlo[12,21−23]and molecular dynamics simulations.[24,25] Patel and Tirrel have correlated their experimental data on tethered PS−PVP diblock and PVP−PS−PVP triblock copolymers into a universal curve, using the scaling approach.

Most of the theories described above are based on the lattice model, which has the inherent limitation that it does not account for the stiffness of the polymer chains. Moreover, it requires that the size of the polymer segment to be same as that of the solvent molecule. Hence, the model overestimates both the configurational entropy of the chain as well as polymer−solvent mixing entropy. Consequently, it is expected to predict a higher interaction energy between the tethered polymer layers. Wijmans et al.[26] have incorporated the chain stiffness into standard lattice theory by assigning different energies to different conformations of a segment on a lattice. Several different schemes of assigning these energies have been discussed. The method has been used for estimating volume fraction profile of the polymer grafted on a single plate. However, the efficacy of the method in predicting energy of interaction between the tethered polymer layers has not yet been evaluated.

The analytical approaches use strong stretching approach which is valid at high grafting densities. However in actual situations, the grafting densities achieved are quite low (in the range of 1−3 mg·m^{-2}). In such situations, the effect of the chain stiffness is more pronounced, and it is shown here that the volume fraction profile of the polymer between the plates at closer approach is no longer parabolic. Strong stretching approach is not valid in such cases.

In the present study, we have examined the energy of interaction between the two approaching surfaces, bearing grafted chains, using the continuum model.[27] The model is based on the mean field SCF theory. The assumption of mean field holds very well since the tethering density of chains is very high. The chain segments are assumed to obey the Boltzmann statistics under the self-consistent field potential of the surface. The stiffness of the chain is accounted for using the random flight model and the modified Flory−Higgins theory is used to accommodate the difference in the volume of the polymer segment and the solvent molecule. The model incorporates the constraint that the total number of chains in the grafted layer is constant and that one end (or both ends) of each chain lies on the solid surface. Moreover, the model can also account for the asymmetric situation where for example, the polymer is grafted only on one of the two plates and the other plate is bare.

The model has been validated by comparing the predicted force−distance profiles with those experimentally determined by other workers using the surface force apparatus. The experimental data used for the validation span cases like chains tethered on both the plates, chains tethered only on one of the two plates and tethered loops. We have found that among all the variables, the tethered amount has the strongest influence on the force−distance profile. Unfortunately, in most experiments, the values of the tethered amount have not been reported. Hence it was regressed from the force−distance profiles. Only in one case is the tethered amount reported, and our estimate closely matches with the reported value.[2] We have also found that the regression estimates of the tethered amount are consistent with the expected trend. Especially for long chains, the dependence of the tethered amount on the chain length matches with that predicted by Currie et al.[1] using the box model of AdG.

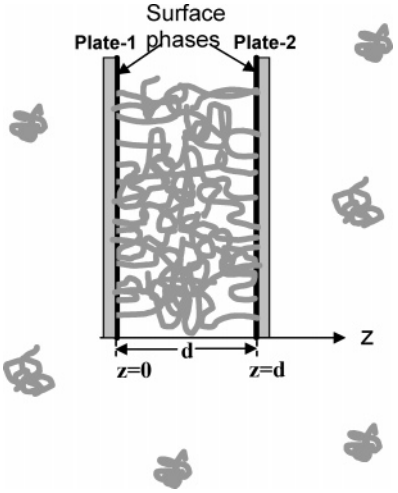

Figure 1. Schematic diagram of the system. F represents the force required to hold the plates at distance d from each other.

We have also compared the volume fraction profiles and the force distance profile of our model with the lattice based SF model using the equivalent chain approach. It is shown that in order to obtain a quantitative estimate of the force−distance profile, it is necessary to account for the effect of chain stiffness and the segment−solvent size difference.

The Model

A continuum form of the self-consistent field theory has been used to describe the configurational statistics of the polymer chains at the solid−liquid interface. Here, we consider a grafted layer of polymer in the gap between two plane-parallel plates (numbered 1 and 2), in contact with an infinite quantity of the solution containing a monodisperse polymer dissolved in a monomeric solvent (see Figure 1). The plates are assumed to be large in size so that the edge effects can be neglected. The model can account for the situation where the two plates differ in their surface properties and hence have different affinities for the adsorbing species. We calculate the total free energy of the system as a function of the distance d between the plates.

The polymer layer is assumed to consist only of the pendent block and the solvent. The tethering block is assumed to be a part of the surface. Moreover, it is assumed to modify the property of the surface but not its topology. Thus, the surface remains a plane even after the adsorption of the tethering block. It is also assumed that the thickness of the layer formed by the tethering block is very small compared to d, the distance between the plates, and hence it is neglected in computing the distance between the approaching surfaces.

We assume the pendent block to be a homopolymer having r freely joined segments each of length l. We

conceptualize three regions of the polymer layer, two surface phases located at $z = 0$ and $z = d$, which consist of polymer segments and solvent molecules in direct contact with the surface, and the interphase, which fills rest of the gap between the plates. For the sake of simplicity, a surface phase is assumed to be two-dimensional (i.e., with zero thickness, but having a finite mass of the adsorbed species). The potential of the field exerted by the solid on the fluid phase is assumed to be confined only to the surface phase. Hence, there is a discontinuity in the potential between the surface phase and the adjoining location in the interphase, although both lie at $z = 0$. To distinguish these two locations, the surface phase is denoted by an asterisk. The surface phase is assumed to be in equilibrium with the interphase. The concentrations in the bulk solution and the interphase are described by volume fractions (ϕ_p for the polymer and ϕ_s for the solvent) whereas those in the surface phases are described by area fractions (φ_p^* and φ_s^*).

A heuristic approach has been used to obtain the free energy of the system. This is discussed in detail elsewhere.[28] In this approach, the chemical potential of a polymer segment at any location in the interphase, and also in the surface phase, is expressed as the sum of homogeneous and nonhomogeneous contributions. The latter arises due to the potential gradient existing in the interfacial region that is transmitted to the segment through chain connectivity. The homogeneous contribution is estimated using the local composition of the solution. For monomeric solvent molecules, only the homogeneous contribution exists. The expression describing the total Helmholtz free energy of the system, which includes the contributions from the bulk solution, the interphase and the surface phase, is written in terms of chemical potentials of the species and the equations describing the constraints are added using the Lagrange multipliers. The constraints are (i) that the total number of molecules in the system is constant, (ii) that the volume fractions of the solvent and the polymer species add to unity in the bulk and at each location in the interphase, (iii) that the area fractions add to unity in each of the two surface phases, and (iv) that the amount of the tethered polymer is constant and is equal to the prespecified value, Γ.

The total free energy is subjected to variational minimization with respect to the volume fraction profiles and the area fractions. The resulting equations can be solved to obtain the relations between nonhomogeneous and homogeneous contributions to the chemical potential of polymer segment. Elimination of the nonhomogeneous contribution from the free energy expression reduces it to the following form:

$$f_i = \frac{V^b}{A_s}\left(\frac{\phi_p^b}{v_p}\mu_p^b + \frac{\phi_s^b}{v_s}\mu_s^b\right) + \int_0^d \left[\frac{\phi_p}{v_p}\left(\mu_p^b - \frac{v_p}{v_s}\mu_s^b\right) + \left(\frac{\mu_s^h}{v_s}\right)\right] dz + \left[\frac{\varphi_{p1}^*}{a_p}\left(\mu_p^b - \frac{a_p}{a_s}\mu_s^b\right) + \frac{\mu_{s1}^{h\,*}}{a_s}\right] + \left[\frac{\varphi_{p2}^*}{a_p}\left(\mu_p^b - \frac{a_p}{a_s}\mu_s^b\right) + \frac{\mu_{s2}^{h\,*}}{a_s}\right] - \tau\Gamma \quad (1)$$

In the above expression, f_i represents the free energy of interaction per unit area of the surface of one plate. The superscript b corresponds to the bulk solution. V^b is the volume of the bulk solution. The variables ϕ_p and μ_s^h refer to the interphase. The chemical potentials μ_s^h (in the interphase) and μ_p^{h*} and μ_s^{h*} (in the surface phase) are the homogeneous contributions. Partial volume of the solvent molecule is v_s and the partial area is a_s. The corresponding quantities for polymer segment are v_p and a_p. The quantity τ is the Lagrange multiplier, used for imposing the constraint that the quantity of the tethered polymer is equal to Γ.

$$\Gamma = \int_0^d \left(\frac{\phi_p(z) - \phi_p^f}{v_p}\right) dz + \frac{\varphi_{p1}^*}{a_p} + \frac{\varphi_{p2}^*}{a_p} \quad (2)$$

Γ represents the tethered amount expressed in terms of the number of polymer segments per unit area of the plate. The term ϕ_p^f represents the volume fraction of free chains, i.e., those that are not tethered to the plates. These chains enter the gap through the bulk material. Since the concentration of the polymer bulk solution is often very low, the contribution of these chains to the total volume fraction is insignificant. Hence the ϕ_p^f term is neglected in eq 2.

It is also customary to express the tethered amount in terms of the dimensionless tethering density σ, which represents the ratio of the actual number of the tethered chains to maximum number of chains that could be tethered. The tethering density σ is related to Γ by the following equation:

$$\sigma = \frac{\Gamma v_p}{rl} \quad (3)$$

The expression for the mean field potential acting on the polymer segment is obtained by subtracting entropy part, $(kT/r) \ln \phi_p$ from the nonhomogeneous contribution to the chemical potential of the polymeric species. Thus

$$u_p(z) = (\mu_p^h - \mu_p^b) - \frac{v_p}{v_s}(\mu_s^h - \mu_s^b) - \frac{kT}{r}\ln\frac{\phi_p}{\phi_p^b} + \tau \quad (4)$$

$$u_p^* = (\mu_p^{h*} - \mu_p^b) - \frac{v_p}{v_s}(\mu_s^{h*} - \mu_s^b) - \frac{kT}{r}\ln\frac{\varphi_p^*}{\phi_p^b} + \tau \quad (5)$$

The terms u_p and u_p^* represent the potentials of the polymer segment in the interphase and the surface phase respectively, relative to that in the bulk. The homogeneous contributions to the chemical potentials (μ_p^h, μ_s^h) in the interphase are calculated using the Flory−Huggins theory.

$$\mu_p^h = \frac{1}{r}\ln\phi_p + \left(\frac{1}{r} - \frac{v_p}{v_s}\right)(1 - \phi_p) + \frac{v_p}{v_s}\chi(1 - \phi_p)^2 \quad (6)$$

$$\mu_s^h = \ln(1 - \phi_p) + \left(1 - \frac{v_s}{rv_p}\right)\phi_p + \chi\phi_p^2 \quad (7)$$

Combining eqs 4, 6, and 7, we obtain

$$u_p(z) = -kT\left(\frac{v_p}{v_s}\right)\left[\ln\left\{\frac{1 - \phi_p(z)}{1 - \phi_p^b}\right\} + 2\chi\{\phi_p(z) - \phi_p^b\}\right] + \tau \quad (8)$$

The corresponding potentials in the two surface phases are obtained from eq 8, by replacing the volume fractions ϕ_p and ϕ_s by the corresponding area fractions φ_p^*

and φ_s^* and adding the surface affinity parameters χ_1^* and χ_2^* Thus

$$u_{p1}^* = -kT\frac{a_p}{a_s}\left[\ln\left\{\frac{1-\varphi_{p1}^*}{1-\phi_p^b}\right\} + 2\{\chi\varphi_{p1}^* - \chi\phi_p^b\}\right] - \chi_1^* + \tau \quad (9)$$

$$u_{p2}^* = -kT\frac{a_p}{a_s}\left[\ln\left\{\frac{1-\varphi_{p2}^*}{1-\phi_p^b}\right\} + 2\{\chi\varphi_{p2} - \chi\phi_p^b\}\right] - \chi_2^* + \tau \quad (10)$$

The configuration statistics of a tethered chain is described by a random flight model.[27] The probability weight of finding a chain segment, with contour coordinate q, at a location z, is the joint probability weight of the two events $E_t(z,q)$ and $E_f(z)$. $E_t(z)$ is the event that the weighted walk of length q starting from the tethered end terminates at z and $E_f(z)$ is the event that weighted walk of length $rl - q$ starting from the free end terminates at z. We define the contour coordinate of a segment as the distance measured from a specified chain end (tethered end in the above example) along the chain contour to the point at which the segment is located.

The probability weight, $G_p(z,q|j)$ that a walk of contour length q, beginning from the chain-end j, terminates at location z can be written in the form of the following recurrence relation:

$$G_p(z,q|j) = e^{-u_p(z)/kT}\left[\frac{1}{4\pi l^2}\int_S G_p(z_s, q-l|j)\, dS\right] \quad (11)$$

Here, S is the surface of the sphere of radius l, centered at z.

The above equation can be expanded in a Taylor series, with respect to both z and q, with appropriate truncations, to yield the following partial differential equation

$$l\frac{\partial G_p(z,q|j)}{\partial q} = \frac{l^2}{6}\frac{\partial^2 G_p(z,q|j)}{\partial z^2} + [1 - e^{u_p(z)/kT}]G_p(z,q|j) \quad (12)$$

Alternatively, if we expand eq 11 only in z, we get

$$G_p(z,q|j) = e^{-u_p(z)/kT}\left[G_p(z,q-l|j) + \frac{l^2}{6}\frac{d^2 G_p(z,q-l|j)}{dz^2}\right] \quad (13)$$

Both the above forms of the model equation are equivalent. Equation 12 is a partial differential equation, whereas eq 13 is a difference differential equation. Both yield the same numerical solution. In the form of eq 13, we can show the equivalence of the random flight model to the lattice model as follows. If we expand the second derivative in z in eq 13 in the finite difference form, we obtain

$$G_p(z,q|j) = e^{-u_p(z)/kT}\left[G_p(z,q-l|j) + \frac{l^2}{6\Delta z^2}\{G_p(z-\Delta z,q-l|j) - 2G_p(z,q-l|j) + G_p(z+\Delta z,q-l|j)\}\right] \quad (14)$$

where Δz is the node spacing. If in eq 14, we use $\Delta z = l$, we obtain

$$G_p(z,q|j) = e^{-u_p(z)/kT}[\lambda_1 G_p(z-l, q-l|j) + \lambda_0 G_p(z,q-l|j) + \lambda_1 G_p(z+l, q-l|j)] \quad (15)$$

where $\lambda_1 = 1/6$ and $\lambda_0 = 1 - 2\lambda_1 = 2/3$.

Equation 15 is the representation of the simple cubic lattice model, with lattice spacing l. Thus, the simple cubic lattice model is equivalent to the present random flight model provided the chain flexibility is such that the correlation length l equals the lattice spacing Δz.

The surface boundary condition for our random flight model is obtained from the following recurrence relation.[27]

$$G_p(0,q|j) = e^{-u_p(0)/kT}\left[\frac{1}{4\pi l^2}\int_{S_h} G_p(z_h, q-l|j)\, dS_h + G_p^*(q-l|j)\right] \quad (16)$$

The boundary condition 16 expresses the constraint imposed on the chain configuration due to the impenetrability of the solid surface. S_h represents the surface of hemisphere, centered at $z = 0$ and having radius l. $G_p(0,q|j)$ is the probability that the walk ends at $z = 0$ and $G_p^*(q - l|j)$ is the probability the walk ends in the surface phase. The two are related as follows

$$\frac{G_p^*(q|j)}{G_p(0,q|j)} = e^{-[u_p^* - u_p(0)]/kT} \quad (17)$$

Using the Taylor expansion and appropriate truncation, eqs 16 and 17 can be converted to either the partial differential equation

$$l\frac{\partial G_p(0,q|j)}{\partial q} = (1 + 2e^{(u_p(0)-u_p^*)/kT})^{-1}\left[\frac{l}{2}\frac{\partial G_p(z,q|j)}{\partial z}\Big|_{z=0} + G_p(0,q|j)\{1 - 2e^{u_p(0)/kT} + 2e^{(u_p(0)-u_p^*)/kT}\}\right] \quad (18)$$

or the difference differential equation

$$G_p(0,q|j) = e^{-u_p(0)/kT}\left[G_p(0,q-l|j)\left(\frac{1}{2} + e^{-[u_p^* - u_p(0)]/kT}\right) + \frac{l}{4}\frac{\partial G_p(z,q-l|j)}{\partial z}\Big|_{z=0}\right] \quad (19)$$

For a nonadsorbing chain: $u_p^*/kT \to \infty$. In this case eq 19 transforms to

$$G_p(0,q|j) = e^{-u_p(0)/kT}\left[\frac{1}{2}G_p(0,q-l|j) + \frac{1}{4}\frac{\partial G_p(z,q-l|j)}{\partial z}\Big|_{z=0}\right] \quad (20)$$

By writing the derivative term in the above equation in the difference form, we obtain

$$G_p(0,q|j) = e^{-u_p(0)/kT}\left[\frac{1}{2}G_p(0,q-l|j) + \frac{1}{4\Delta z}\{G_p(\Delta z,q-l|j) - G_p(0,q-1|j)\}\right] \quad (21)$$

Using $\Delta z = l$, the above equation is converted to a form,

which resembles the boundary condition of the lattice model

$$G_p(0,q|j) = e^{-u_p(0)/kT}[\lambda_0^* G_p(0,q-l|j) + \lambda_1^* G_p(l,q-l|j)] \quad (22)$$

In the above equation, $\lambda_1^* = 1/4$ and $\lambda_0^* = 1/2 - \lambda_1^* = 1/4$. Note that these are not the coordination numbers of the simple cubic lattice. In this respect the continuum model differs from the lattice model. For adsorbing chains, the number λ_0^* in eq 22 is modified to $\lambda_0^* = 1/4 + \exp[-\{u_p(0) - u_p^*\}/kT]$. This will result in a further deviation from the lattice model.

The rest of the boundary and the initial conditions required to solve the random flight equation are case specific. We consider the following four cases.

Case 1. Single Plate with Tethered Chains. This case arises when the two plates carrying the chains are far apart so that the chains from one plate do not interact with those from the other plate. Hence we can take each plate separately. The z-coordinate varies from $z = 0$ to $z = d$, where d is chosen sufficiently long so as to allow complete extension of the chains. The pertinent initial conditions for the free and the tethered ends are, respectively, as follows:

$$G_p(z,0|f) = e^{-u_p/kT} \quad (23)$$

$$G_p(z,0|t) = M\delta(z) \quad (24)$$

where $\delta(z)$ is the Dirac delta function and M is a large, positive, but otherwise arbitrary number. The condition given by eq 24 forces the tethered end to remain at $z = 0$.

The boundary condition corresponding to $z = d$ for eq 12 is

$$l\frac{\partial G_p(d,q|j)}{\partial q} = \left[-\frac{l}{2}\frac{\partial G_p(z,q|j)}{\partial z}\Big|_{z=d} + G_p(d,q|j)(1 - 2e^{u_p(d)/kT})\right] \quad (25)$$

and for eq 13 it is

$$G_p(d,q|j) = e^{-u_p(d)/kT}\left[\frac{1}{2}G_p(d,q-l|j) - \frac{l}{4}\frac{\partial G_p(z,q-l|j)}{\partial z}\Big|_{z=d}\right] \quad (26)$$

The volume fraction of the polymer at location z in the interphase and its area fraction in the surface phase are obtained by the following equations:

$$\phi_p(z) = \frac{\phi_p^b}{rl}e^{u_p(z)/kT}\int_0^{rl} G_p(z,q|t)G_p(z,rl-q|f)\,dq \quad (27)$$

$$\varphi_p^* = \frac{\phi_p^b}{rl}e^{u_p^*/kT}\int_0^{rl} G_p^*(q|t)G_p^*(rl-q|f)\,dq \quad (28)$$

We assume no density change accompanying the exchange of molecules between the solution and the surface phase. This requires that

$$\frac{a_p}{a_s} = \frac{v_p}{v_s} \quad (29)$$

The total quantity of polymer in the gap, in terms of the number of segments per unit area of one plate is given by

$$\Gamma = \int_0^d \left(\frac{\phi_p(z)}{v_p}\right)dz + \frac{\varphi_p^*}{a_p} \quad (30)$$

Case 2. Two Plates with Tethered Chains. The Symmetric Case. In this case two identical parallel plates with identically tethered chains interact with each other. The mid-plane symmetry allows us to consider only half the domain, i.e., from $z = 0$ to $z = d/2$, where d is the distance between the plates. Since both plates are identical $\chi_1^* = \chi_2^* = \chi^*$. The relevant equations and the boundary/ initial conditions are same as that of case 1 except that the boundary condition given by eq 25 is replaced by the mid-plane symmetry condition

$$\frac{\partial G_p(z,q|j)}{\partial z}\Big|_{z=d/2} = 0 \quad (31)$$

The total amount of the polymer in the gap is computed by the following equation

$$\Gamma = 2\int_0^{d/2}\left(\frac{\phi_p(z)}{v_p}\right)dz + \frac{2\varphi_p^*}{a_p} \quad (32)$$

Case 3. Two Plates with Chains Tethered on Only One Plate. In this case the chains are tethered on the plate placed at $z = 0$. The other plate does not have any tethered chains on it. We use the full domain i.e., from $z = 0$ to $z = d$. The equations are identical to case 1 except for the boundary condition given by eqs 18 and 25 which are replaced by the following equations:

$$l\frac{\partial G_p(0,q|j)}{\partial q} = (1 + 2e^{(u_p(0)-u_{p1}^*)/kT})^{-1}\left[\frac{l}{2}\frac{\partial G_p(z,q|j)}{\partial z}\Big|_{z=0} + G_p(0,q|j)\{1 - 2e^{u_p(0)kT} + 2e^{(u_p(0)-u_{p1}^*)/kT}\}\right] \quad (33)$$

$$l\frac{\partial G_p(d,q|j)}{\partial q} = (1 + 2e^{(u_p(d)-u_{p2}^*)/kT})^{-1}\left[-\frac{l}{2}\frac{\partial G_p(z,q|j)}{\partial z}\Big|_{z=d} + G_p(d,q|j)\{1 - 2e^{u_p(d)/kT} + 2e^{(u_p(d)-u_{p2}^*)/kT}\}\right] \quad (34)$$

Equation 17 changes to a set of two equations

$$\frac{G_{p1}^*(q|j)}{G_p(0,q|j)} = e^{-[u_{p1}^*-u_p(0)]/kT}, \frac{G_{p2}^*(q|j)}{G_p(d,q|j)} = e^{-[u_{p2}^*-u_p(d)]/kT} \quad (35)$$

Case 4. Two Plates with Tethered Loops. Symmetric Case. Here both ends of a chain are tethered to a plate, this forming a loop. This case can be treated in a manner similar to case 2 except that the initial conditions given by eqs 23 and 24 are replaced by the following conditions:

$$G_p(z,0|t_1) = M\delta(z) \quad (36)$$

$$G_p(z,0|t_2) = M\delta(z) \quad (37)$$

In the above equations, $t_1$and t_2 represent two tethered

ends of the chain. Equations 27 and 28 are replaced by

$$\phi_p(z) = \frac{\phi_p^b}{rl} e^{u_p(z)/kT} \int_0^{rl} G_p(z,q|t_1) G_p(z,rl-q|t_2)\, dq \quad (38)$$

$$\varphi_p^* = \frac{\phi_p^b}{rl} e^{u_p^*/kT} \int_0^{rl} G_p^*(q|t_1) G_p^*(rl-q|t_2)\, dq \quad (39)$$

Finally the total quantity of the polymer in the gap is computed using eq 32.

For the purpose of comparison of the continuum model with the lattice model, we define the equivalent lattice spacing l_0 as

$$l_0 = l\left(\frac{v_s}{v_p}\right) \quad (40)$$

We preserve the total contour length of the chain and hence the number of segments of the equivalent lattice chain is

$$r_0 = r\left(\frac{l}{l_0}\right) \quad (41)$$

Simulation Procedure. We exemplify the method of simulation with reference to case 1. Other cases can be treated in the similar manner. The equations pertaining to the configurational statistics have been cast in two different forms, i.e., as partial differential equation (eq 12) or as a difference-differential equation (eq 13). The partial differential form can be converted into a set of linear ordinary differential equations in q using finite element method. These equations can be solved using eigenvalue analysis to yield the chain configuration and the volume fraction profile of the polymer. To solve the difference-differential eq 13, it is first cast in the finite difference form by discretizing the z domain and the resulting difference equation can be solved by matrix method. Although, both the methods yield the same numerical results, each has a distinct advantage. The first method is much faster than the second for very long chains. However, it becomes numerically unstable for simulation of the extended configurations of tethered chains. The second method (based on difference differential equations) is useful in this situation. Hence for case 1(case of a single plate), we have used the second method, whereas for all other cases we have used the first method.

Since the first method is described in detail elsewhere,[27] we do not describe it here. Instead, we describe the method involving the difference-differential equation. To solve the difference-differential eq 13, it is first cast in the difference form by discretizing the z domain into N intervals of equal width and converting the derivatives with respect to z to the finite difference form.

$$G_p(z_i,\hat{q}|j) = e^{-u_p(z_i)/kT}[\lambda_1 G_p(z_{i-1},\hat{q}-1|j) + \lambda_0 G_p(z_i,\hat{q}-1|j) + \lambda_1 G_p(z_{i+1},\hat{q}-1|j)] \quad (42)$$

where z_i is the ith node in the z domain ($i = 1,2,..., N-1$) and

$$\hat{q} = \frac{q}{l}, \quad \Delta z = \frac{d}{N}, \quad \lambda_1 = \frac{l^2}{6\Delta z^2}, \quad \text{and } \lambda_0 = 1 - \frac{l^2}{6\Delta z^2} \quad (43)$$

The boundary conditions at $z = 0$ (eq 19) transform to

$$G_p(z_0,\hat{q}|j) = {}^{-u_p(z_0)/kT}[\lambda_0^* G_p(z_0,\hat{q}-1|j) + \lambda_1^* G_p(z_1,\hat{q}-1|j)] \quad (44)$$

where

$$\lambda_0^* = \frac{1}{2} - \frac{l}{4\Delta z} + \exp[-\{u_p(z_0) - u_p^*\}/kT] \text{ and } \lambda_1^* = \frac{l}{4\Delta z} \quad (45)$$

The boundary condition at $z = d$ (eq 26) transforms to

$$G_p(z_N,q|j) = e^{-u_p(z_N)/kT}[\lambda_1{}^d G_p(z_{N-1},\hat{q}-1|j) + \lambda_0{}^d G_p(z_N,\hat{q}-1|j)] \quad (46)$$

where

$$\lambda_0{}^d = \frac{1}{2} - \frac{l}{4\Delta z}, \lambda_1{}^d = \frac{l}{4\Delta z} \quad (47)$$

Equations 42, 44, and 46 are combined and written in the following matrix form

$$\vec{G}_p(\hat{q}|j) = \vec{C}\vec{G}_p(\hat{q}-1|j) \quad (48)$$

where $\vec{G}_p(\hat{q}|j)$ is a vector $\{G_p(z_i,\hat{q}|j),\ i = 0, 1, ..., N\}$, containing the probability weights of the segments and the matrix is the connectivity matrix, which relates the probability weights of the adjacent segments. It can be written as

$$\vec{C} = \begin{bmatrix} \lambda_0^* e^{-u_p(z_0)/kT} & \lambda_1^* e^{-u_p(z_0)/kT} & 0 & \cdots & 0 & 0 & 0 \\ \lambda_1 e^{-u_p(z_1)/kT} & \lambda_0 e^{-u_p(z_1)/kT} & \lambda_1 e^{-u_p(z_1)/kT} & \cdots & 0 & 0 & 0 \\ \vdots & \vdots & \vdots & \cdots & \vdots & \vdots & \vdots \\ 0 & 0 & 0 & \cdots & 0 & \lambda_1{}^d e^{-u_p(z_N)/kT} & \lambda_0{}^d e^{-u_p(z_N)/kT} \end{bmatrix} \quad (49)$$

The solution of eq 48 is

$$G_p(\hat{q}|j) = \vec{C}^r \vec{G}^r{}_p(\hat{q}=0|j) \quad (50)$$

Here, $\vec{G}_p(\hat{q}=0|j)$is the vector of probability weights for $q = 0$. For the tethered end

$$\vec{G}_p(\hat{q}=0|t) = \{M,0,0,...,0\} \quad (51)$$

and for the free end

$$\vec{G}_p(q=0|f) = \{e^{-u_p(z_0)/kT}, e^{-u_p(z_1)/kT}, ..., e^{-u_p(z_N)/kT}\} \quad (52)$$

The volume fraction of the polymer at a node is computed by the following equation

$$\phi_p(z_i) = \frac{\phi_p^b}{r} e^{u_p(z_i)/kT} \sum_{q=0}^{r} G_p(z_i,\hat{q}|t) G_p(z_i,r-\hat{q}|f) \quad (53)$$

The area fractions in the surface phase are computed using the following equation

$$\varphi_p^* = \frac{\phi_p^b}{r} e^{u_{p^*}/kT} \sum_{q=0}^{r} G_p^*(\hat{q}|t) G_p^*(r-\hat{q}|f) \quad (54)$$

where $G_p^*(\hat{q}|t)$is related to $G_p(z_0,q|j)$ by the following equation

$$\frac{G^*_{p1}(q|j)}{G_p(z_0,q|j)} = e^{-[u_{p^*}-u_p(z_0)]/kT} \tag{55}$$

To solve these equations, we need $u_p(z)$ and u^*_p. These quantities can be computed using eqs 8 and 9. The value of τ is so chosen that eq 30 is satisfied for the prespecified value of Γ. Since the volume fractions and area fractions are not known a priori, an iterative solution is required. After the converged values of the volume and the area fractions are obtained, the free energy per unit area is computed using eq 1.

Although, one can solve the above equations using the fictitious reference state approach described by Wijmans et al.,[13] the present method of using the Lagrange parameter τ has some distinct advantages. The present method does not require rescaling of the probability weights as is the case with the fictitious reference state approach. Moreover, using the converged value of the Lagrange parameter, the free energy of the system can be directly computed using eq 1. A more elaborate procedure is needed for computing free energy using the fictitious reference state approach.

The free energy of compression, $f_c(d)$, per unit area of one plate is given by

$$f_c(d) = f_i(d) - f_i(d_c) \tag{56}$$

The energy is related to the force of compression in the surface force apparatus by Derjaguin approximation

$$F(d) = 2\pi R f_c(d) \tag{57}$$

where R is the radius of the crossed cylinders. Force−distance profile is a plot of F/R vs d.

Estimation of Model Parameters

The model has several parameters. Most of them could be estimated apriori. Since the experimental data reported in the literature pertains to polystyrene-toluene system, with mica as the solid surface, parameter estimation is done with reference to this system.

The correlation length of polystyrene is obtained from the radius of gyration under Θ condition, using the method described in the literature.[17] Using the following relation between the radius of gyration R_g and molecular weight of the polymer, M_p

$$R_g(\text{nm}) = 0.0280\sqrt{M_p} \tag{58}$$

the estimated value of l is 1.61 nm. Also, one polymer segment (of length l) contains 5.23 repeat units.

The partial molar volume of a species (solvent/polymer) is assumed to be equal to the molar volume of the pure component in amorphous state and is estimated from the density values. The estimated molar volumes for various components at 298 K are as follows: PS (segment), 0.518 dm^3 mol; toluene, 0.106 dm^3 mol.[29] From these, v_p and v_s are estimated.

For polystyrene in toluene (good solvent), the value of the Flory−Huggins parameter χ is 0.40 at 295 K[17] and is assumed to be independent of the concentration of polystyrene. The values of χ at other temperatures are estimated, using the Θ temperature of the PS−toluene system, which is 119 K.[30]

It is known that the polystyrene does not adsorb on mica from toluene at ambient temperatures, hence a large negative value is used for the interaction parameter χ^* between polystyrene and bare mica. However when mica surface is grafted, the grafted moiety changes the surface characteristics of mica. In general the tethering moiety, e.g., poly(ethylene oxide), is neither compatible with PS nor toluene. In this case, the value of χ^* can be uncertain and hence cannot be estimated a priori. Fortunately, the energy of interaction between the tethered chains is practically insensitive to the choice of χ^* as shown later. Hence, any value can be used for χ^*. In the present simulation, the value used is $\chi^* = 0$.

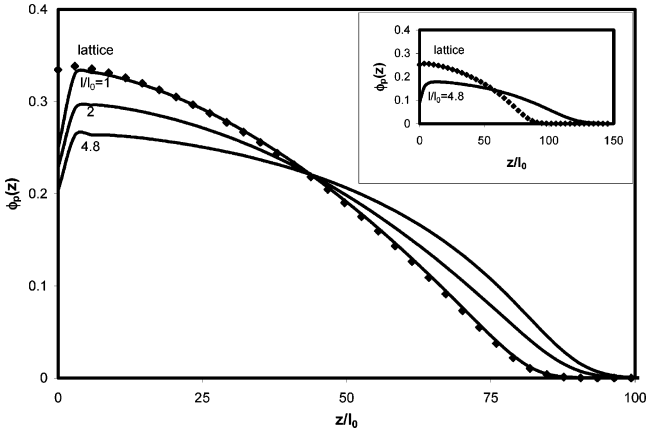

Figure 2. Volume fraction profile of polymer grafted to a single nonadsorbing plate: Comparison of between the lattice and the continuum models. The points represent the lattice model whereas the solid lines represent continuum model for different values of chain flexibility, l/l_0. The abscissa is the distance from the plate scaled by the lattice spacing. Parameters are $r_0 = 176$, $\chi = 0$ and $\sigma = 0.1$. Inset: the same plot for longer chain and lesser tethered amount. Parameters: $r_0 = 510$, $\chi = 0$, and $\sigma = 0.013$. The points represent the lattice model and the solid line represents the continuum model with $l/l_0 = 4.8$.

Another parameter in the model is the area occupied by the solvent on the mica surface (a_s). We can relate a_s to the packing factor f for the solvent as

$$a_s = f N_{av}^{1/3} v_s^{2/3} \tag{59}$$

where N_{av} is the Avogadro number. Packing factor is defined as the ratio of the projected area of a solvent molecule on a plane surface to the area of the face of a cube having the same volume as that of the molecule. It is a measure of the effectiveness of packing of molecules at the surface compared to that in the solution. For a spherical molecule projecting on the surface as a circle, the value of f is 1.2. Since no direct measurement of f is possible, we have used $f = 1.2$ in our simulations. It is shown later that the energy of interaction is also insensitive to f.

Results and Discussion

Figure 2 presents the volume fraction profiles, for nonadsorbing chains tethered on a single plate (case 1). They are computed using the continuum model (bold lines) and compared with the simple cubic lattice model (filled squares). The continuum chains with different stiffness are simulated. All the profiles are parabolic. The continuum model profile for $l/l_0 = 1$ matches very well with that of the lattice model, except for a small deviation very close to the plate. This is expected as per the discussion in the section pertaining to the model.

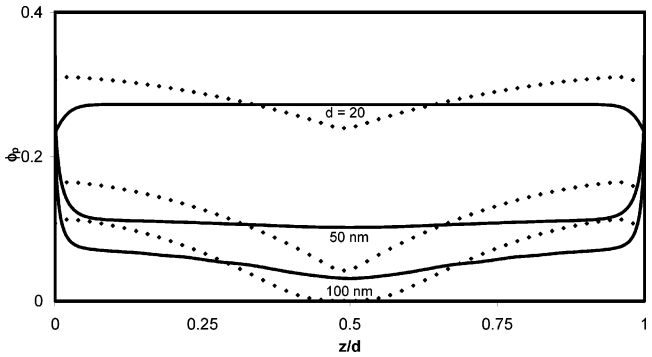

Figure 3. Volume fraction profile of polymer in the gap between two parallel plates: Comparison between lattice model (points) and continuum model (solid lines). Polymer is symmetrically tethered on both the plates, with one end of each chain anchored to the surface. The abscissa is normalized distance (z/d). The parameters used are: Continuum model l = 1.61 nm, r = 260, χ = 0.4, χ^* = 0, Γ = 3.0 mg/m^2, f = 1.2. The parameters for the equivalent lattice chains are l_0 = 0.335 nm, r_0 = 1235, χ = 0.4, χ^* = 0, Γ = 3.0 mg/m^2, and $\sigma = 7.0 \times 10^{-3}$.

As the chain stiffness increases, the continuum model deviates from the lattice model as seen in the figure. A stiffer chain is seen to be more extended and to compensate for this extension it shows a lower peak value of the volume fraction. The effect of chain stiffness is more pronounced at lower tethered amounts as seen from the inset of the figure. Here, the tethering density is about one-eighth of that in the main figure. The chain length is appropriately increased in order to maintain nearly the same extension of the lattice chain as in the main figure. The continuum chain with stiffness factor 4.8 is seen to be significantly more extended than the lattice chain. The stronger effect of the stiffness at low tethering densities is expected since in this case the chains are less crowded and try to attain their natural configuration.

Figure 3 shows the volume fraction profiles of a polymer tethered symmetrically on two plates (case 2) as a function of the normalized distance (z/d) between the plates. The parameters used for the simulation are listed in the figure. It is seen from the figure that, except for a small region near the plate, the volume fraction profiles of the continuum chain are flat in the entire gap. Thus, the profiles have brushlike characteristics. On the other hand, the profiles of the equivalent lattice chains are distinctly parabolic. The reason for this difference is that as the tethering density is low, the continuum chains (l/l_0 = 4.8) are well extended. This also results in a greater interpenetration of chains between the two polymer layers. We also see that at larger separations, the continuum model predicts a higher concentration of the polymer at the surface than that in the brush. This happens because, as per our model, for χ^* = 0, the polymer adsorption on the plate surface is entropically favorable.[27]

It is also seen from the profiles that the polymer retains a large quantity of the solvent even when the plates are very near each other ($1 - \phi_p \approx 0.75$ for d = 20 nm). This behavior is expected under good solvent conditions used in the simulation.

Figures 4−8 show the effect of various parameters on the force−distance profiles for case 2. All the profiles show repulsion, which increases with decreasing distance. Among these parameters, the three most important are the tethered amount Γ, the polymer−solvent interaction parameterχ and chain length r. The energy of interaction increases with increase in the tethered amount and decreases with increase in the χ parameter. These trends are expected. With increase in the tethered amount, more solvent has to leave the gap for a specified distance between the plates. This generates higher osmotic pressure in the gap. With an increase in the value of χ, the solvent drains more easily and hence the osmotic pressure is lowered.

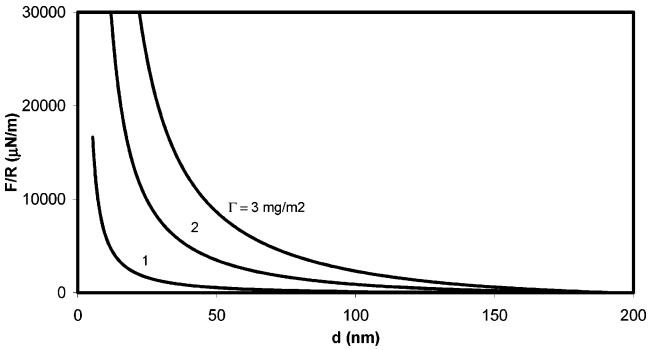

Figure 4. Effect of the tethered amount, Γ, on the force−distance profile. Values of Γ (mg/m^2) = 1.0, 2.0, 3.0. Other parameters used are l = 1.61 nm, r = 1000 (∼550 kDa), χ = 0.4, χ^* = 0, and f = 1.2.

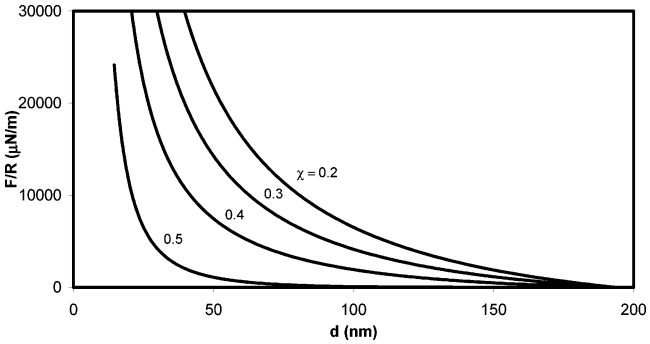

Figure 5. Effect of the polymer−solvent interaction parameter, χ, on the force−distance profile. Values of χ = 0.2, 0.3, 0.4, 0.5. Other parameters used are l = 1.61 nm, r = 1000 (∼550 kDa), χ^* = 0, f = 1.2, and Γ = 3.0 mg/m^2.

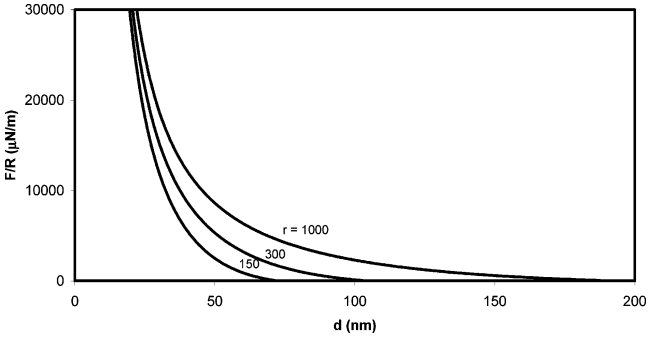

Figure 6. Effect of chain length, r, on force−distance profile. Values of r = 150, 300, 1000. Other parameters used are l = 1.61 nm, χ = 0.4, χ^* = 0, f = 1.2, and Γ = 3.0 mg/m^2.

Since the chain length affects the distance of onset of interaction, its effect is more pronounced at long distances between the plates (see Figure 6). As the total amount of the polymer in the gap is same for all the curves in this figure, all the curves converge when the gap narrows down. Thus, the short distance part of the force−distance profile is less sensitive to chain length. From this, we can also deduce that polydispersity would affect the shape of the profile only for large values of d.

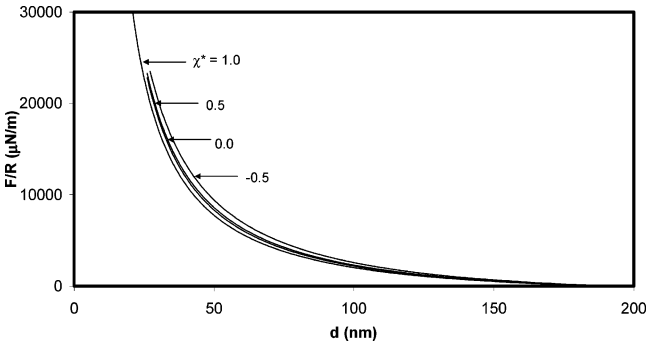

Figure 7. Effect of the polymer−surface interaction parameter, χ^* on force−distance profile. Values of $\chi^* = -0.5$, 0, 0.5, 1.0. Other parameters used are $l = 1.61$ nm, $r = 1000$ (∼550 kDa), $\chi = 0.4$, $f = 1.2$, and $\Gamma = 3.0$ mg/m^2.

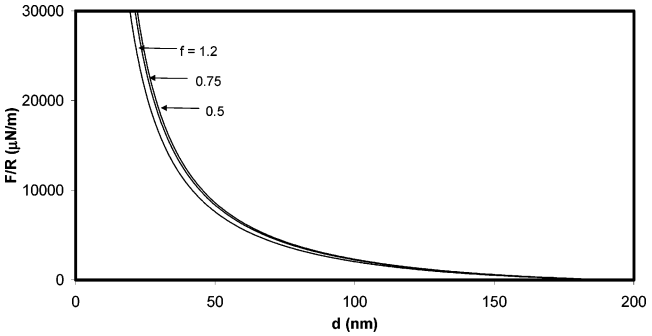

Figure 8. Effect of the packing factor, f, on the force−distance profile. Values of $f = 0.5$, 1.0, 1.2. The other parameters used are $l = 1.61$ nm, $r = 1000$, $\chi = 0.4$, $\chi^* = 0$, and $\Gamma = 3.0$ mg/m^2.

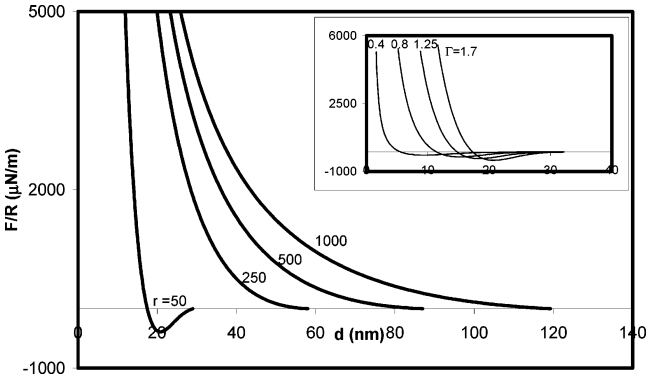

Figure 9. Effect of the chain length, r, on the force−distance profile for a tethered loop. Values of $r = 50$, 250, 500, 1000. Other parameters used are $l = 1.61$ nm, $\chi = 0.38$, $\chi^* = 0$, $f = 1.2$, $\Gamma = 1.7$ mg/m^2, and temperature = 305 K. Inset: the effect of tethered amount on force−distance profiles at a fixed chain length ($r = 50$). Values of Γ (in mg/m^2) = 0.4, 0.8, 1.25, 1.7. Other parameters are the same as mentioned above.

The surface affinity parameter χ^* and the packing factor, f has very small effect on the force−distance profiles as shown in Figures 7 and 8. The reason for this insensitivity is that the surface phase contribution to the total energy is very small. Because of this insensitivity, the lack of accurate estimates of these parameters will not affect the prediction of the energy profiles.

Figure 9 represents the force−distance profile of interacting loops. It is seen that for long loops, the profile is repulsive, but for short loops (e.g., for a loop with 50 segments) it is attractive. For the latter case, the attraction begins when plates are at a distance of about 35 nm. The length of the chain of 50 segments is 80 nm. This means the distance between the plates is

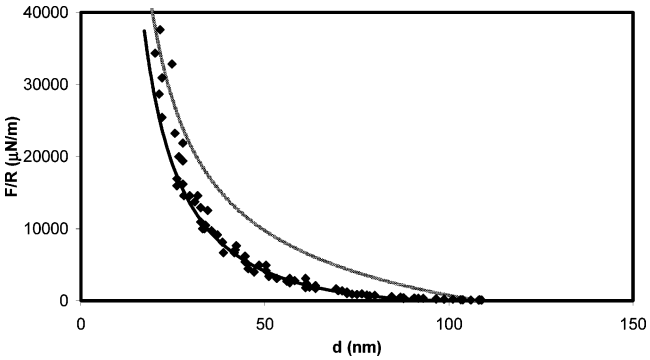

Figure 10. Force−distance plot for PS−X 140 kDa. Comparison of the continuum model theory (bold line) and the lattice model (lighter line) with the experiments[2] at 298 K (points). The tethered amount is reported as 3.0 ± 0.5 mg/m^2. The parameters used are as follows: for the continuum model, $l = 1.61$ nm $r = 260$, $\chi = 0.4$, $\chi^* = 0$, $\Gamma = 3.0$ mg/m^2, and $f = 1.2$; for the equivalent lattice chains, $l_0 = 0.335$ nm, $r_0 = 1235$, $\chi = 0.4$, $\chi^* = 0$, and $\Gamma = 3.0$ mg/m^2.

nearly equal to half the length of the chain forming the loop. Since these short loops are highly constrained, they have very low configurational entropy. The entropy of mixing makes important contribution to the total entropy. When the loops penetrate each other the entropy of mixing increases. This causes lowering of the energy. This conjecture can be further supported by comparing the force−distance profiles as a function of the tethered amount (see the inset of Figure 9). It is observed that the tethered amount is decreased, not only the energy dip becomes shallower, but the onset of attraction shifts to lower distances. The reason for this is, with the lowering of the tethered amount, the entropy of mixing decreases and hence loops have to penetrate deeper before it becomes significant. It is also found that the profile is only slightly sensitive to χ^*, indicating that the contribution of bridging to the attractive part of the energy is insignificant.

For validating the model for cases 2 and 3, we have used the experimental results of Taunton et al.[2] Here, polystyrene chains are grafted on to mica surface using two techniques. In the first technique, the grafting is through a reactive (zwitterionic) end group ($-CH_2)_3N^+(CH_3)_2-(CH_2)_3SO_3-$) on polystyrene chains. In the second, a short poly(ethylene oxide) block at the end of the polystyrene chain is used. Both these techniques yield the similar force−distance profiles. We have used both types of the data for comparison. In one of their experiments, the tethered amount has been estimated using the measurement of the refractive index of the material in the gap. Figure 10 compares the model prediction (case 1) with experimentally measured profile, for polystyrene of molecular weight 140 kDa. The reported tethered amount is 3 ± 0.5 mg·m^{-2} on each of the two plates. We have used the value of 3.0 mg·m^{-2} in the model. The model matches well with the experimental data.

The lighter line in the above figure is the force−distance profile of the equivalent lattice chain. It is seen from the plot that the lattice model overestimates the force at longer distances. The difference between the model and the experiment reduces at shorter distances. Since the lattice chain has larger number of segments, it yields higher mixing entropy as well as the configurational entropy. Hence there is a greater loss of entropy when the plates are brought together. At shorter distances, steric repulsion dominates and hence the

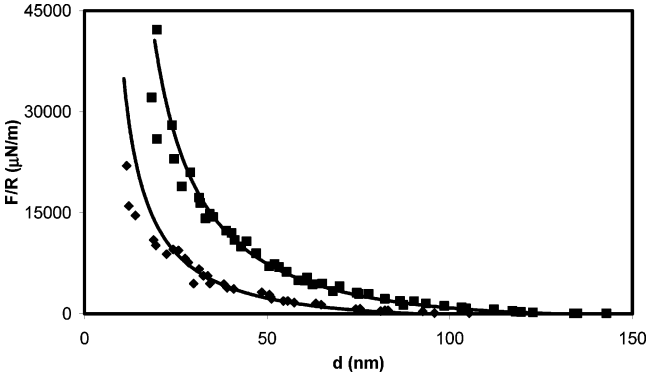

Figure 11. Force−distance plot for PS−PEO (PS block of 150 kDa). Comparison of the theory (solid line) with the experiments (points)[2] at 298 K. Two cases are considered. In the first, the polymer is tethered to both the plates (curve to the right). In the second, polymer is tethered only on one of the plates. Parameters used in the simulation are $\chi = 0.4$, $\chi^* = 0$, $f = 1.2$, and $\Gamma = 3.0$ mg/m^2 on each plate for the first case and on one of the two plates for the second case.

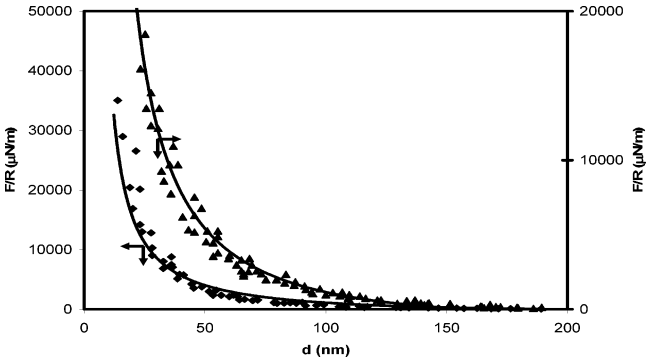

Figure 12. (Left) Force−distance plot for PS−X 375 kDa. (Right) Energy−distance plot for PS−X 660 kDa. Comparison of the continuum model (solid line) with the experiments (points)[2] at 298 K. The estimated tethered amounts are $\Gamma = 2.5$ mg/m^2 for PS−X 375kDa and $\Gamma = 2.1$ mg/m^2 for PS−X 660 kDa; the other parameters are $\chi = 0.4$, $\chi^* = 0$, and $f = 1.2$.

difference between the experiment and model narrows down.

Figure 11 presents comparison of the continuum model with the experiments, for cases 2 and 3. Both the experiments are done with the same polymer,[2] i.e., diblock copolymer PEO-*b*-PS (with short chain of PEO) having molecular weight of 150 kDa (of the PS block). The curve to the right corresponds to case 2 where the grafting density is equal on both the plates, whereas in the other curve, grafting is done only on one of the plates. The tethered amount is not reported for both the experiments. However, since the molecular weight of the polymer used is nearly same as that corresponding to Figure 10, we have used 3.0 mg·m^{-2} as the tethered amount. The model predictions are in good agreement with both the experiments.

Figures 12 and 13 compare the continuum model predictions with the experiments for four different molecular weights of the symmetrically tethered polymer. Since the tethered amount is not reported in any of these experiments, it is used as a fitting parameter. Here also the model matches well with the experimental data.

Further confirmation of the model can be obtained by comparing the predicted maximum extension of the polymer layer with that determined experimentally by Taunton et al. These authors have reported the critical

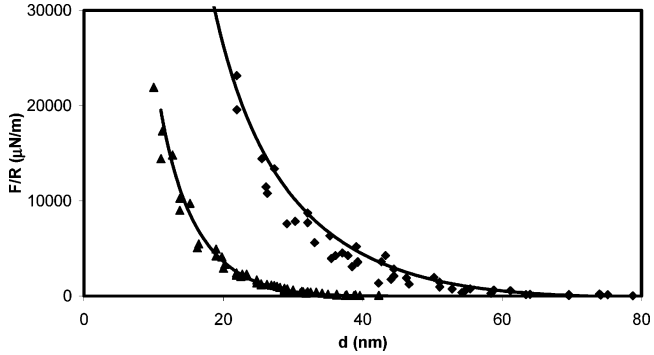

Figure 13. (Left) Force−distance plot for PS−X 26 kDa. (Right) Energy−distance plot for PS−X 58 kDa. Comparison of the continuum model (solid lines) with the experiments (points)[2] at 298 K. The estimated tethered amounts are $\Gamma = 1.94$ mg/m^2, for PS−X 26 kDa. and $\Gamma = 3.0$ mg/m^2, for PS−X 58 kDa. The other parameters are, $\chi = 0.4$, $\chi^* = 0$, and $f = 1.2$.

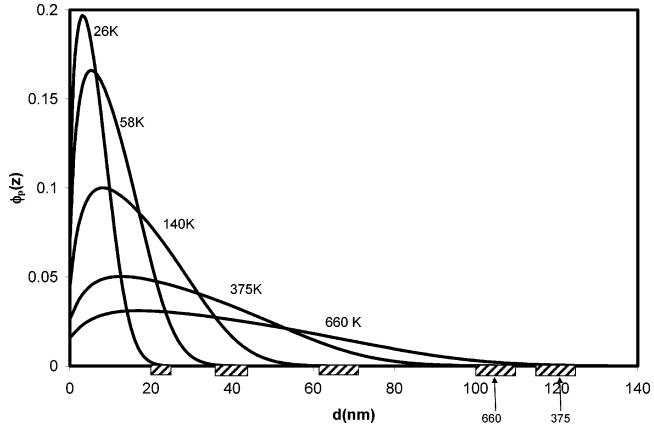

Figure 14. Extension of the chains tethered on a single plate (nonadsorbing) corresponding to the molecular weight and tethered amount as described in Figure 10, 12, and 13. The hatched portion indicates the chain extension reported by Taunton et al.[2] Parameters used: $\chi = 0.4$, Γ (in mg·m^{-2}) = 1.94 (26 K), 3.0 (58 K), 3.0 (140 K), 2.5 (375 K), and 2.1 (660 K).

distance of separation between the plates beyond which the tethered polymer layers cease to interact. Half this distance represents the maximum extension of the polymer layer on a single plate. Figure 14 shows the volume fraction profiles of the chains simulated in Figures 10, 12, and 13. The values of Γ used in the simulations are those previously estimated. The experimental values of the chain extension are marked on the abscissa using hatched lines. It is seen that except for 375 K chain, rest of the chain extensions match with the simulations. The extension of the 375 K chain appears to be abnormally high.

The estimated values of the tethered amount are plotted against the molecular weight of the polymer in Figure 15. It is seen that for long chains, the estimated values of the tethered amount decrease with increase in the molecular weight of the polymer. Using the box model of AdG, Currie et al.[1] have shown that for the case of constant adsorption energy per chain, the number of chains grafted per unit area of the surface is proportional to $r^{-3/2}$. Since there are r segments per chain, the amount of the polymer grafted per unit area of the plate is proportional to $r^{-1/2}$ i.e. directly proportional to its radius of gyration. The assumption of the constant adsorption energy per chain is valid for the experimental data presented here since tethering is

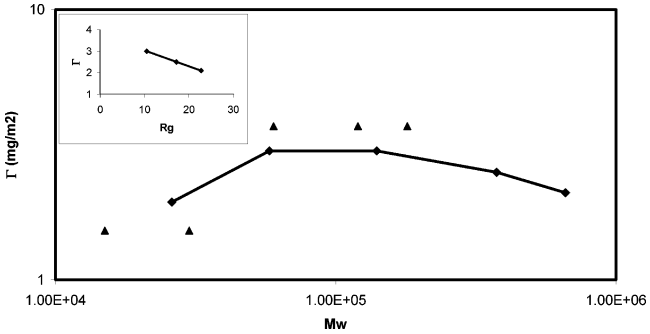

Figure 15. Double logarithmic plot of tethered amount vs the molecular weight of polymer. (◆) Tethered amounts for one-end tethered chains, estimated from the force−distance profiles in Figure 10 and Figures 12−13, using the model. (▲) Tethered amounts for grafted loops are estimated from the force−distance profiles of Figure 16. Tethered amounts for the loops are multiplied by 2 to facilitate comparison with one-end tethered chains. Inset: Plot of tethered amount vs R_g for long chains with one-end tethered.

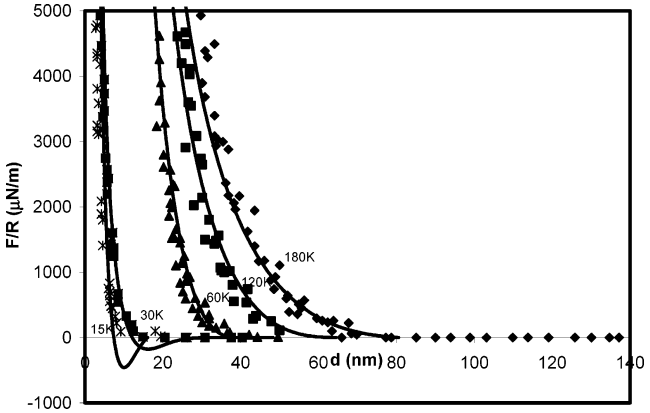

Figure 16. Energy-distance plot for PVP−PS−PVP triblock copolymers for different molecular weights of PS block.[7] The temperature is 305 K. Points represents the experimental results and continuous lines represent the respective model predictions. Molecular weights of PS block = 180, 120, 60, 30 and 15 kDa. The molecular mass of the PVP block is 30 K in all cases. The model parameters are $\chi = 0.38$, $\chi^* = 0$, and $f = 1.2$. The estimates of tethered amount are $\Gamma = 1.85$ mg/m^2 for 180, 120, and 60 kDa chains and 0.76 for 30 and 15 kDa chains.

done using short tethering blocks which are attached to the surface as trains. In the inset of Figure 15, we have plotted the values of Γ for long chains against R_g. The plot is a straight line. This indicates that our estimates are consistent with the trend predicted by the box model.

For shorter chain lengths, the dependence of the tethered amount on the chain length is quite different, the tethered amount decreases with decreasing chain length. This happens because for very short chains, we expect the graft density to reach a constant value, in which case the tethered amount should vary directly with r.

For validating case 4, i.e., that pertaining to tethering of loops, we have used the experiments reported by Patel and Tirrel[7] for the triblock copolymers, PVP-*b*-PS-*b*-PVP, tethered on mica surface. The model fits are shown in Figure 16. The fits are good for polymers with PS-block molecular weight in the range of 60 to 180 kDa (first three curves from the right). For shorter loops, the model predicts attraction, whereas the actual profile is repulsive at all distances. A possible reason for this deviation is that in these cases, the length of the pendent block is much shorter then the total length of the tethering block. Hence even a small degree of interaction between these two blocks can substantially alter the force−distance profile. In such case, the pendent blocks will not extend and the attractive interaction will be absent.

The estimated tethered amount is plotted against the molecular weight of the pendent block in Figure 15 (filled triangles). In the case of loops, since two anchoring blocks are present, per chain, we expect, for the same surface coverage, half the amount of pendent polymer present in the tethered layer compared to the chain with single tethering block. Hence, to facilitate comparison with the one-end tethered chains, the tethered amount is doubled and plotted against the molecular weight of PS block. It appears to follow a trend similar to that corresponding to one-end tethered chains.

Conclusions

Using the continuum model we have been able to successfully predict the force−distance profiles for two plates carrying end tethered polymer. The predicted profiles closely follow the experimental profiles. In the experiment where the tethered amount is measured, estimated tethered amount is in close agreement with the measured value. In the rest of the cases, it follows a consistent trend. The critical distance of interaction, predicted by the model is also in good agreement with the experiments. Moreover, the effects of various parameters on the force−distance profile, predicted by the model, are in agreement with our qualitative understanding of the theory. The only serious deviation from the experiments is in the case of short tethered loops, where the theory predicts attractive minimum in the force−distance, whereas the experiments show monotonic increase. We feel that the theory deviates from the experiments because it ignores the interaction between the pendent loop and the tethering blocks, which is likely to be present in the real situation.

We have also shown that the present theory accounts for both the stiffness of the chain and the difference in the volume of the Kuhn segment and that of the solvent molecule.

The present model cannot predict the equilibrium tethered amount since it does not take into account the energy associate with adsorption of the tethering block. To obtain a more accurate insight into the problem, it would be necessary to incorporate the tethering block in the present analysis. This would also be necessary if the force−distance profiles for the short loops are to be reconciled with the theory.

Acknowledgment. The authors would like to thank (i) Unilever Research India for providing the financial support and (ii) Mr. V. M. Naik and Dr. S. J. Suresh of Unilever Research India for their valuable suggestions.

References and Notes

(1) Currie, E. P. K.; Norde, W.; Cohen Stuart, M. A. *Adv. Colloid Interface Sci.* **2003**, *100−102*, 205.
(2) Taunton, H. J.; Toprakcioglu, C.; Fetters, L. J.; Klein, J. *Macromolecules* **1990**, *23*, 571.
(3) Taunton, H. J.; Toprakcioglu, C.; Fetters, L. J.; Klein, J. *Nature (London)* **1988**, *332*, 712.
(4) Dai, L.; Toprakciouglu, C. *Macromolecules* **1992**, *25*, 6000.

(5) Hadziioannou, G.; Patel, S.; Granick, S.; Tirrel, M *J. Am. Chem. Soc.* **1986**, *108*, 2869.
(6) Kelly, T. W.; Schorr, P. A.; Johnson, K. D.; Tirrel, M.; Frisbie, C. D. *Macromolecules* **1998**, *31*, 4297.
(7) Patel, S.; Tirrel, M.; Hadziioannou, G. *Colloids Surf.* **1988**, *31*, 157.
(8) Israelachvili, J. N.; Tirrel, M.; Klein, J.; Almog, Y. *Macromolecules* **1984**, *17*, 204.
(9) Hu, H.-W.; Granick, S. *Macromolecule*s **1990**, *23*, 613.
(10) Alexander, S. *J. Phys. (Paris)* **1977**, *38*, 983.
(11) de Gennes, P. G. *Macromolecules* **1980**, *13*, 1069.
(12) Cosgrove, T.; Heath, T.; van Lent, B.; Leermakers, F.; Scheutjens, J. *Macromolecules* **1987**, *20*, 1692.
(13) Wijmans, C. M.; Scheutjens, J. M. H. M.; Zhulina, E. B. *Macromolecules* **1992**, *25*, 2657.
(14) Martin, J. I.; Wang, Z.-G. *J. Phys. Chem.* **1995**, *99*, 2833.
(15) Wijmans, C. M.; Zhulina, E. B.; Fleer, G. J. *Macromolecules* **1994**, *27*, 3238.
(16) Wijmans, C. M.; Factor, B. J. *Macromolecules* **1996**, *29*, 4406.
(17) Fleer, G. J.; Cohen Stuart, M. A.; Scheutjens, J. M. H. M.; Cosgrove, T.; Vincent, B. *Polymers at Interfaces*; Chapman and Hall: London, 1993.
(18) Milner, S. T.; Witten, T. A.; Cates, M. E. *Macromolecules* **1988**, *21*, 2610.
(19) Milner, S. T. *J. Chem. Soc., Faraday Trans.* **1990**, *86*, 1349.
(20) Zhulina, E. B.; Borisov, O. V.; Priamitsyn, V. A. *J. Colloid Interface Sci.* **1990**, *137*, 495.
(21) Chakrabarti, A.; Toral, R. *Macromolecules* **1990**, *23*, 2016.
(22) Dickman, R.; Anderson, P. E. *J. Chem. Phys.* **1993**, *99*, 3112.
(23) Pepin, M. P.; Whitmore, M. D. *J. Chem. Phys.* **1999**, *111*, 10381.
(24) Murat, M.; Grest, G. S. *Macromolecules* **1991**, *24*, 704.
(25) Seidel, C.; Netz, R. R. *Macromolecules* **2000**, *33*, 634.
(26) Wijmans, C. M.; Leermakers, F. A. M.; Fleer, G. J. *J. Chem. Phys.* **1994**, *101*, 8214.
(27) Juvekar, V. A.; Anoop, C. V.; Pattanayek, S. K.; Naik, V. M. *Macromolecules* **1999**, *32*, 863.
(28) Pattanayek, S. K.; Juvekar, V. A. *Macromolecules* **2002**, *35*, 9574.
(29) Perry, R. H.; Green, D. W. *Perry's Chemical Engineering handbook*, 7th ed.; McGraw-Hill, New York, 1997; pp 2−95.
(30) Schuld, N.; Wolf, E. A. In *Polymer Handbook*, 4th ed.; Brandrup, J., Emmergut, E. H., Grulke, E. A., Eds.; John Wiley and Sons Inc.: New York, 1999; p 7/304.

MA048319H